Oncology and Translational Medicine
DOI 10.1007/s10330-015-0113-9

August 2015, Vol. 1, No. 4, P146–P151

ORIGINAL ARTICLE

Acquired renal arteriovenous malformation: the diagnostic value of three-dimensional multidetector-row computed tomography*

Qiuxia Wang[1], Liang Chen[2], Xuemei Hu[1], Yao Hu[1], Daoyu Hu[1], Zhen Li[1] (✉)

[1] Department of Radiology, Tongji Hospital, Tongji Medical College, Huazhong University of Science and Technology, Wuhan 430030, China
[2] Department of Radiology, Binzhou Medical University Hospital, Binzhou 256603, China

Abstract

Objective To evaluate the diagnostic value of three-dimensional multidetector-row computed tomography (MDCT) in detecting acquired renal arteriovenous malformation (RAVM) and to compare its performance with that of ultrasonography and digital subtraction angiography (DSA).

Methods The institutional review board approved this retrospective study and written informed consent was obtained from all patients before examination. All 14 patients with acquired RAVM underwent MDCT, including cortical and medullary phase enhancement angiography and three-dimensional (3D) reconstruction. Five and nine patients were further examined and their diagnoses confirmed by DSA and surgery, respectively. The MDCT images, including 3D reconstructions, were analyzed for RAVM independently and in consensus by two observers using a workstation.

Results Among the 14 patients with acquired RAVM, 12 with maximum lesion diameter ≥ 10 mm, and one with a maximum lesion diameter between 5 and 10 mm, were correctly diagnosed with MDCT angiography. Among these patients, four diagnoses were confirmed by DSA. One patient with a lesion 5–10 mm in diameter was misdiagnosed with a renal aneurysm by MDCT angiography. The other one with the maximum diameter of the lesion between 5 mm and 10 mm was misdiagnosed as renal aneurysm with MDCT angiography, which was diagnosed as renal arteriovenous malformation with DSA. Among 14 lesions in 14 patients, eight and six originated in the left and right kidney, respectively.

Conclusion MDCT angiography can accurately diagnose RAVM and improve our understanding of the disease, which will allow clinicians to provide better care.

Received: 19 June 2015
Revised: 9 July 2015
Accepted: 5 August 2015

Key words: arteriovenous malformation; kidney; multidetector row computed tomography; digital subtraction angiography

With the development of renal biopsy and improved treatment modalities for renal trauma, the incidence of acquired renal arteriovenous malformation (RAVM) has gradually increased in recent years [1–4]. Most cases are unilateral and characterized by direct communications between renal arteries and veins via enlarged, tortuous vascular spaces. The symptoms of RAVM usually include hematuria, vascular masses, and intractable hypertension [5–8]. Although digital subtraction angiography (DSA) has long been considered the reference standard for diagnosis of RAVM [9], it is an invasive technique less useful as a conventional means to screen patients suspected of having RAVM.

With advances in multidetector-row computed tomography (MDCT) technology, MDCT angiography offers improved spatial resolution and has replaced traditional imaging work up, including DSA, for most visceral arteries [10–11]. Compared to traditional axial CT, maximum intensity projection (MIP), volume rendering (VR), multiplanar volume reconstruction (MPVR), and three-dimensional (3D) reconstruction MDCT imaging can offer more detailed visualization of vascular disorders.

✉ Correspondence to: Zhen Li. Email: zhenli@hust.edu.cn
* Supported by grants from the National Natural Science Foundation of China (No. 81271529), the Natural Science Foundation of Hubei Province (No. 2014CFB298) and the Health and Family Planning Research of Hubei Province (No. WJ2015MB066).

Thus, this study retrospectively analyzed and compared MDCT angiography imaging data to that of DSA for diagnosis of acquired RAVM.

Materials and methods

Patients

This study was approved by the review board of Tongji Hospital at Tongji Medical College of the Huazhong University of Science and Technology, and written informed consent was obtained from all patients before examination. From September 2006 to July 2012, double phase contrast enhanced MDCT was routinely performed according to a local protocol on patients with suspected RAVM based on ultrasound findings and clinical features. Among these, 14 patients (10 women and 4 men; age range, 13–54 years; mean age, 34.71 ± 13.57 years), each with an RAVM lesion at least 5 mm in diameter (mean diameter, 34.79 ± 19.99 mm; range, 6–81 mm), were retrospectively included in our study group. All patients had a history of percutaneous renal biopsy or penetrating trauma, and were clinically normal before the examinations. None of these subjects had concomitant renal cancer or other renal diseases. Five patients were further examined by DSA and all cases were confirmed as RAVM by DSA or surgery at Tongji Hospital.

MDCT evaluation

MDCT scans of all patients were performed with a 64-detector MDCT (LightSpeed VCT, GE Healthcare Technologies, USA). The intravenous contrast protocol was 80–100 mL of nonionic contrast medium (Iopamiro 370 mg/mL, Brocco Sine, Shanghai, China) and physiological saline injected into the antecubital vein with an 18 gauge intravenous cannula using a double tube high-pressure injector (Stellant, Medred Co., USA) at a rate of 4 mL/s.

Patients were in a supine position. The MDCT scanning parameters were as follows: tube voltage 120 kV; tube current 150–440 mA; rotation time 0.5 s; detector pitch 1.375 : 1; detector rows 64 mm × 0.625 mm; matrix 512 × 512; table speed 39.37 mm/rotation; and slice thickness/interval 0.625 mm.

Renal cortical phase scanning was initiated by bolus tracking (Smartprep, GE Healthcare Technologies) when a threshold enhancement of 120 Hu was reached in the abdominal aorta [12–13]. Medullar phase imaging was initiated 15 s after completion of arterial phase scanning.

DSA evaluation

Using the Seldinger technique, a 5F Yahsiro polyethylene catheter was placed in the main renal artery to obtain a baseline selective angiography with cut film or digital subtraction techniques (Toshiba-2000 DSA system, Toshiba, Japan). The DSA parameters were as follows: tube voltage 66 kV; tube current 400 mA; exposure frequency 15 p/s. The intra-arterial contrast protocol included 35–45 mL of Iohexol (Omnipaque 350 mg/mL, GE Healthcare Technologies) injected using a high-pressure injector (Stellant, Medred Co., USA) at a rate of 3–4 mL/s.

Image analysis

All MDCT image data were processed on a workstation (Advantage Windows 4.3; GE Medical Systems). Double phase MDCT images were independently analyzed by two radiologists (DY.H. and Z.L, with 27 and 12 years of experience, respectively, of reporting abdominal CT findings) at a GE Advantage Windows 4.3 workstation.

The source axial enhancement images were reconstructed using the ADW4.3 protocol. We reconstructed the kidney for three-dimensional (3D) analysis by volume rendering (VR), multiplanar volume reconstruction (MPVR), maximum intensity projection (MIP), and (3D) reconstruction technique. The combined source images were assessed for signs of RAVM and the findings compared to retrospective MDCT angiography and DSA findings.

Statistical analysis

MDCT angiography and DSA images were retrospectively analyzed and data compared using Fisher's exact test (SPSS Statistics for Windows, Version 17.0., SPSS Inc., Chicago, IL). *P* values less than 0.05 were considered statistically significant.

Results

Among 14 lesions from 14 patients, eight and six lesions originated from the left and the right kidney, respectively. Eight lesions were located in the junction between the renal cortex and medulla; four were giant, and some abnormal vessels were located beside the kidney. Two lesions were located in the inferior renal pole, and were complicated with angiomyolipoma (Table 1 and Fig. 1).

Of the 14 patients, 12 with lesions of maximum diameter greater than 10 mm, and one with a 5–10 mm maximum lesion diameter, were correctly diagnosed with RAVM by MDCT angiography. Diagnoses in four of these patients were confirmed by DSA. One additional patient, with a 5–10 mm diameter lesion, was misdiagnosed with renal aneurysm by MDCT angiography (Fig. 2), a finding confirmed by DSA (Table 1).

Both MDCT angiography and DSA showed thickened, circuitous, and well-defined arterial and venous elements as well as cavernous channels. In one case, the thickened and circuitous vein filled with contrast medium in the arterial phase – also visible by DSA – was incorrectly con-

Table 1 Diagnosis and therapy of 14 patients with acquired RAVM

No.	Sex/age	Diagnosis	Therapy	Origin	Cause	Size of AVM (mm)		
						CTA	DSA	Surgery
1	M/19	MDCTA	Surgery	LK	PRB	13	–	17
2	F/25	MDCTA	Surgery	RK	PRB	35	–	32
3	M/52	MDCTA	Surgery	RK	PT	58	–	55
4	F/49	MDCTA & DSA	DSA	LK	PRB	19	18	–
5	F/38	MDCTA	Surgery	RK	PT	34	–	37
6	F/45	MDCTA	Surgery	LK	PRB	32	–	30
7	M/24	MDCTA & DSA	DSA	LK	PT	79	81	–
8	F/53	MDCTA & DSA	DSA	RK	PT	43	44	–
9	F/31	MDCTA	Surgery	LK	PT	51	–	50
10	F/29	MDCTA	Surgery	LK	PRB	38	–	36
11	M/37	MDCTA & DSA	DSA	RK	PT	–	6	–
12	F/51	MDCTA	Surgery	LK	PRB	18	–	20
13	F/18	MDCTA	Surgery	LK	PT	45	–	48
14	F/15	MDCTA & DSA	DSA	RK	PRB	9	9	–

AVM, arteriovenous malformation; MDCTA, 64-detector MDCT angiography; DSA, digital subtraction angiography; LK, left kidney; RK, right kidney; PRB, percutaneous renal biopsy; PT, penetrating trauma

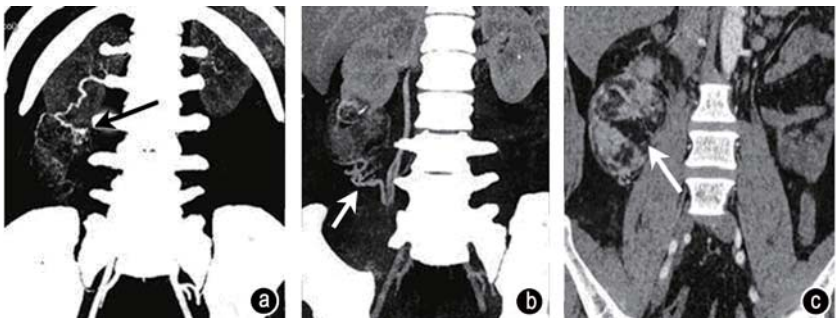

Fig. 1 MIP-3D of cortical phase (a) and intravenous phase (b) images showing AVM of the right kidney, complicated with angiomyolipoma, inferior lobe artery feeding (short arrow in A) the AVM (long arrow in A), and circuitous vein (white arrow in B) draining to right renal vein. Coronal MPVR image shows the lesion fat element (white arrow in C). These findings were confirmed by subsequent surgery. MIP-3D, maximum intensity projection (3 dimensional); AVM, arteriovenous malformation; MPVR, multiplanar volume reconstruction

sidered evidence of renal aneurysm by MDCT angiography.

DSA can measure the speed and pressure of blood flow in AVM. MDCT angiography, on the other hand, can show the whole shape and surrounding structures.

Among the 14 patients included in this study, nine had continuous hypertension and macroscopic hematuria, three had continuous hypertension and microscopic hematuria, and two had microscopic hematuria. In addition, a renal vascular bruit was present in one patient. Hematuria disappeared after surgical and DSA-assisted repair. Hypertension resolved in eight patients after surgical and DSA-assisted repair (Table 2).

Discussion

RAVM is usually classified as aneurysmal or cirsoid [1]. Aneurysmal RAVM is characterized by solitary arteriovenous communications, with single, scrotiform channels, and well-defined arterial and venous elements. In contrast, cirsoid types are considered the true congenital form and are characterized by multiple vascular communications, typically near the collecting system [2–3]. The latter, also called acquired RAVM are the most common and occur as a result of penetrating trauma, percutaneous renal biopsy, and nephrectomy [2, 14–17].

The main symptoms include continuous or intractable hypertension and hematuria (microscopic or macroscopic); the hypertension severity appears to be correlated with the size of the arteriovenous malformation [3]. Vascular mass may be the only finding during health examinations.

Renal vascular bruits are rare signs, found only in relatively large RAVM. One patient had mega-malformation of the left kidney and showed this rare sign of the disorder (Fig. 3). After surgical or DSA-assisted repair, signs typically disappear or diminish. At four-month follow-up examinations after treatment, hematuria, hypertension, and renal vascular bruit had resolved in all patients, eight patients, and one patient, respectively (Table 2). DSA is the accepted reference standard for diagnosis of RAVM; it can clearly show lesion number, size, and location, especially for small malformations. In addition to its use as a diagnostic technique, DSA is also a good treatment option for RAVM [9, 15–19] (Fig. 4). The features of RAVM in conventional CT include masses of vascular density located

Table 2 Comparison of multidetector-row computed tomography angiography and DSA findings

Item	CTA	DSA
No. of case	14	5
Signs		
Fed artery	–	+
Varicose configured vessel	+	+
Draining vein	+	+
Early venous drainage	–	+
Surrounding structures	+	–
Complication	+	–
Diagnosis*		
No. of positive cases	13	5
No. of negative cases	1	0
Reference standard		
DSA	5	5
Surgery	9	0

* Fisher's exact test, $P = 0.304$; +, full view; −, lack of full view; DSA, digital subtraction angiography; CTA, multidetector-row computed tomography angiography

in the renal sinus and surrounding the pelvicalyceal system. Renal and left gonadal vein dilation are also sometimes observed [19]. However, during conventional CT, enhancement techniques such as the amount of contrast medium and speed of injection can significantly affect diagnosis and differential diagnosis [20–21].

MDCT is considered a dependable and noninvasive tool for assessment of almost all types of vascular disorders [10, 21]. This technique helps to identify anomalous kidney vessels and their courses. However, because RAVM is relatively rare, only a few case reports describe cases of RAVM. In our study, MDCT detected 13 of 14 RAVM lesions, visualizing irregular and varicose vessels and aneurismal dilatation, as well as feeding arteries and draining veins. Furthermore, more anatomic details and surrounding renal structures can be displayed on reformatted CT images [13]. For those patients who choose surgery instead of DSA therapy, MDCT angiography can show more anatomic details and pathological information before surgery. Only one patient with RAVM was misdiagnosed with renal aneurysm by MDCT angiography. The maximum lesion diameter was 6 mm; while imaging showed an abnormal vascular lesion, it did not clearly show nonvascular complications such as angiomyolipoma or renal hematoma. This finding suggests that MDCT may

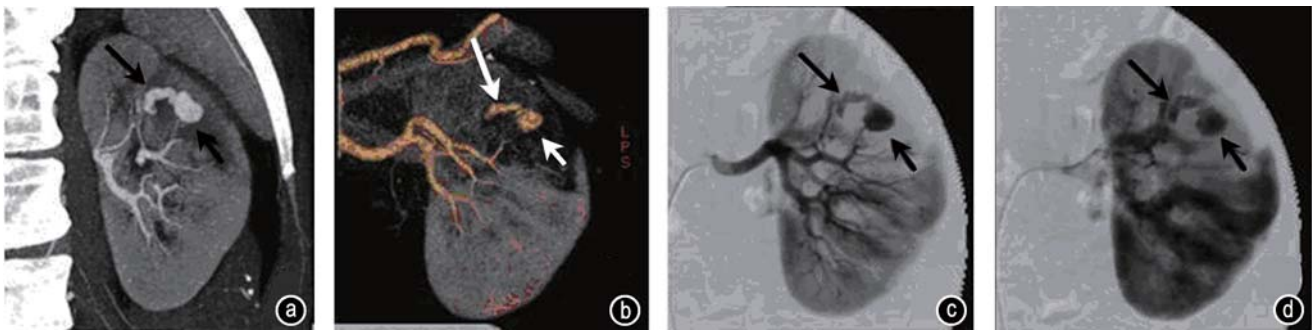

Fig. 2 MIP-3D (A) and VR-3D (b) images misleadingly suggest the lesion to be an aneurysm (short arrow in a, b), and feeding artery (long arrow). Subsequent selective angiography (c, d) images confirm that the feeding arterial actually is a draining vein (long arrow) associated with RAVM; these images also show aneurismal dilatation (short arrow). MIP-3D, maximum intensity projection (3 dimensional); VR-3D, volume rendering (3 dimensional); RAVM, renal arteriovenous malformation

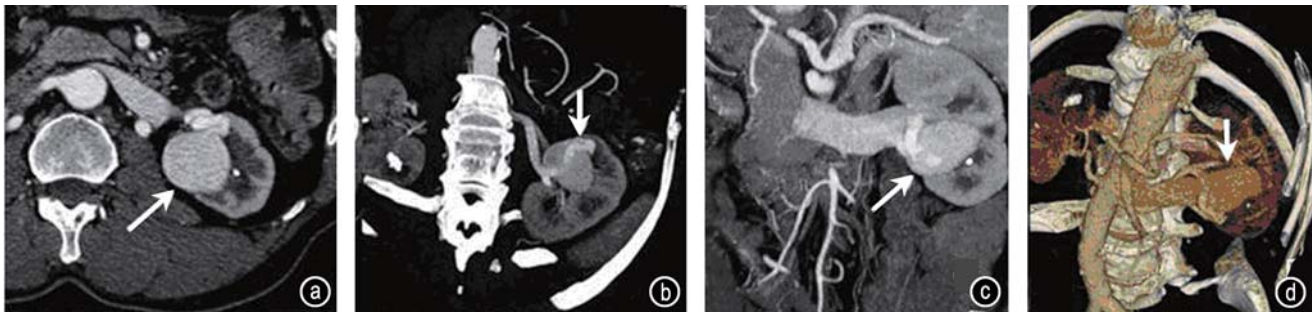

Fig. 3 Left renal AVM (a–d). Gross hematuria without pain had emerged two years prior. Vascular malformation (long arrow) and feeding artery were observed in the cortical phase axial CT images (a). The lesion is visible as a round, bulky vascular malformation. Cortical phase enhancement of maximum intensity projection images (b and c) show AVM and feeding artery (arrow). 3D volume rendering images (d) show the feeding arterial and draining vein associated with RAVM, as well as the aneurismal dilatation (arrow). AVM, renal arteriovenous malformation; RAVM, renal arteriovenous malformation

Fig. 4 Left renal AVM in a 49-year-old woman (a–e). Axial (a) and coronal (b, c) maximum intensity projection CT images show AVM in cortical phase enhancement (short arrow and long arrows). Subsequent selective angiography images (d, e) confirm that the feeding arterial actually is a draining vein associated with RAVM; the images also show aneurismal dilatation (long arrow). AVM, arteriovenous malformation; RAVM, renal arteriovenous malformation

not be as reliable as DSA for diagnosis of small RAVMs (maximum diameter < 10 mm). The reason for this lack of sensitivity may be that the lesion was too small to be displayed well by MDCT. Another reason may be that the double-phase enhancement scans of MDCT are independent processes rather than continuous images as is the case for DSA. DSA can more easily display the continuous movement of blood flow in small RAVMs. However, one case does not provide conclusive evidence, and advanced research is necessary to confirm these observations.

Compared to DSA, MDCT axial source images can be reconstructed as 2D or 3D images, which permits visualization of the number, size, and location of malformations at any projection without repetitive radiation exposure or extra contrast agent burden [12]. MIP-3D imaging can clearly display renal blood vessel circuitry, dilation, and stenosis, as well as the relationship between the lesion and surrounding structures, similar to DSA. VR-3D imaging is a common imaging reconstruction technique that can show large RAVM lesions, including the origin, circuitry, and dilation of anomalous vessels and surrounding structures. MPVR is a 2D imaging technique that can supplement VR to show RAVM shape and size, as well as the wall and lumen structures of abnormal vessels. MDCT angiography is a multidirectional imaging technique better for visualizing normally distributed kidney sub-arteries and anomalous channels between the artery and vein. Data from MDCT angiography are beneficial for future treatment by DSA or surgery.

This study has several limitations. First, because the disease is relatively rare, the study population was small. Second, there was only one small lesion (less than 10 mm) in the group, and this case was misdiagnosed by MDCT. This sample size and observation is too small to definitively conclude that either method is better. Finally, DSA was performed on only five patients, further emphasizing the need for more advanced research.

In conclusion, MDCT achieved results similar to those of DSA for diagnosis of RAVMs in this study, suggesting that 2D and 3D reconstruction imaging can provide additional information for diagnosis. Compared to DSA, MDCT reconstruction imaging is more easily understood by clinical doctors, and is more acceptable in clinical practice as a non-invasive tool. Further study with a larger sample size is required to better determine the role of MDCT in diagnosis of RAVM.

Conflicts of interest

The authors indicated no potential conflicts of interest.

References

1. Kopchick JH, Bourne NK, Fine SW, *et al.* Congenital renal arteriovenous malformations. Urology, 1981, 17: 13–17.
2. Macpherson RI, Fyfe D, Aaronson IA. Congenital renal arteriovenous malformations in infancy. The imaging features in two infants with hypertension. Pediatr Radiol, 1991, 21: 108–110.
3. Takaha M, Matsumoto A, Ochi K, *et al*. Intrarenal arteriovenous malformation. J Urol, 1980, 124: 315–318.
4. Wirth S, Baumann W, Schulte-Wissermann H. Congenital renal arteriovenous malformation (aneurysmal type) in childhood. Eur J Pediatr, 1985, 144: 270–272.
5. Mehta V, Ananthanarayanan V, Antic T, *et al.* Primary benign vascular tumors and tumorlike lesions of the kidney: a clinicopathologic analysis of 15 cases. Virchows Arch, 2012, 461: 669–676.
6. Lazić M, Hadzi-Djokić J, Basić D, *et al.* Congenital arteriovenous fistula of the horseshoe kidney with multiple hemangiomas. Srp Arh Celok Lek, 2012, 140: 508–510.
7. Gorgulu N, Caliskan Y, Yelken B, *et al.* Effects of arteriovenous fistula on clinical, laboratory and echocardiographic findings in renal allograft recipients. Int J Artif Organs, 2011, 34: 1024–1030.
8. Alarcón CM, Cubillana PL, Alemán AC, *et al*. Hematuria due to congenital arteriovenous fistula treated with embolization. Arch Esp Urol, 2011, 64: 994–996.
9. Yakup Y, Bora P, Barbaros C, *et al*. Endovascular management of iatrogenic renal artery aneurysm and arteriovenous fistula. Saudi J Kidney Dis Transpl, 2012, 23: 838–840.
10. Prokop M. Multislice CT angiography. Eur J Radiol, 2000, 36: 86–96.
11. Fleischmann D. Multiple detector-row CT angiography of the renal and mesenteric vessels. Eur J Radiol, 2003, 45: S79–87.
12. Zhang P, Cai G, Chen J, *et al*. Echocardiography and 64-multislice computed tomography angiography in diagnosing coronary artery fistula. J Formos Med Assoc, 2010, 109: 907–912.

13. Lorenzen J, Schneider A, Körner K, *et al*. Post-biopsy arteriovenous fistula in transplant kidney: treatment with superselective transcatheter embolisation. Eur J Radiol, 2012, 81: e721–726.
14. Kałuża B, Ziobrowski I, Durlik M. Surgical procedures not connected with transplantation in patients after kidney or kidney and pancreas transplant with stable function of graft. Pol Przegl Chir, 2012, 84: 196–201.
15. Breza J Jr, Javorka V Jr, Mizickova M, *et al*. Arterio-venous fistula with pseudoaneurysm of renal artery. Bratisl Lek Listy, 2012, 113: 289–292.
16. Hyams ES, Pierorazio P, Proteek O, *et al*. Iatrogenic vascular lesions after minimally invasive partial nephrectomy: a multi-institutional study of clinical and renal functional outcomes. Urology, 2011, 78: 820–826.
17. Barkhausen J, Verhagen R, Müller RD. Successful interventional treatment of renal insufficiency caused by renal artery pseudoaneurysm with concomitant arteriovenous fistula. Nephron, 2000, 85: 351–353.
18. Durack JC, Wang JH, Schneider DB, *et al*. Vena cava filter scaffold to prevent migration of embolic materials in the treatment of a massive renal arteriovenous malformation. J Vasc Interv Radiol, 2012, 23: 413–416.
19. Wetter A, Schlunz-Hendann M, Meila D, *et al*. Endovascular treatment of a renal arteriovenous malformation with Onyx. Cardiovasc Intervent Radiol, 2012, 35: 211–214.
20. Garg N, Kalra M, Friese JL, *et al.* Contemporary management of giant renal and visceral arteriovenous fistulae. J Endovasc Ther, 2011, 18: 811–818.
21. Davidovic L, Dragas M, Cvetkovic S, *et al*. Twenty years of experience in the treatment of spontaneous aorto-venous fistulas in a developing country. World J Surg, 2011, 35: 1829–1834.

DOI 10.1007/s10330-015-0113-9
Cite this article as: Wang QX, Chen L, Hu XM, *et al*. Acquired renal arteriovenous malformation: the diagnostic value of three-dimensional multidetector-row computed tomography. Oncol Transl Med, 2015, 1: 146–151.